Analog-antianalog isospin mixing in ^{47}K β^- decay

Brian Kootte[1], H. Gallop[1,2], C. Luktuke[1,2], J.C. McNeil[3,1], A. Gorelov[1], D. Melconian[4], J. Klimo[4], B.Vargas-Calderon[4], and J.A. Behr[1,3*]

[1] *TRIUMF, 4004 Wesbrook Mall, Vancouver, BC V6T 2A3 Canada*

[2] *U. Waterloo*

[3] *U. British Columbia*

[4] *Cyclotron Institute, Texas A&M*

(Dated: February 23, 2024)

We have measured the isospin mixing of the $I^\pi = 1/2^+$ E_x=2.599 MeV state in nearly-doubly-magic ^{47}Ca with the isobaric analog $1/2^+$ state of ^{47}K. Using the TRIUMF atom trap for β decay, we have measured a nonzero asymmetry of the progeny ^{47}Ca with respect to the initial ^{47}K spin polarization, which together with the β asymmetry implies a nonzero ratio of Fermi to Gamow-Teller matrix elements $y = 0.099 \pm 0.037$. Interpretation as mixing between this state and the isobaric analog state implies a Coulomb matrix element magnitude 93 ± 35 keV. This relatively large matrix element supports a model from the literature of analog-antianalog isospin mixing which predicts large matrix elements in cases involving excess neutrons over protons occupying more than one major shell. The result supports pursuing a search for time-reversal odd, parity-even, isovector interactions using a correlation in ^{47}K β decay.

I. INTRODUCTION

The neutron beta decays to its isobaric analog state, the proton, as does tritium. Many other isotopes undergo beta minus decay to states of same spin I and parity π, but because of the extra Coulomb energy at higher Z, decay to the isobaric analog state is energetically forbidden. So the Gamow-Teller operator dominates, while the Fermi operator linking isobaric analog states is only allowed if some low-lying final state of same I^π is mixed by an isospin-breaking interaction with the excited isobaric analog. We see such isospin breaking in an $I^\pi = 1/2^+$ state in the ^{47}Ca nucleus 80% fed by the beta decay of ^{47}K. Interference between Gamow-Teller and isospin-suppressed Fermi amplitudes produces a small asymmetry of the progeny recoil direction with respect to the initial nuclear spin, which we measure with TRIUMF's Neutral Atom Trap for β decay (TRINAT). Below we obtain a result of $y = g_V M_F / g_A M_{GT} = 0.099 \pm 0.037$ from a weighted average of recoil and beta asymmetries, implying a Coulomb mixing matrix element 93 ± 35 keV.

Since ^{47}Ca and ^{47}K are near closed shells, the single known ^{47}Ca $1/2^+$ state may contain much of the antianalog configuration and is predicted to have a 190 keV mixing matrix element with the analog [1]. Sensitivity to time reversal-odd parity-even (TOPE) inherently isovector [2] N-N interactions through a β-ν-spin correlation is thought to be enhanced in these systems, as the small amount of time reversal is referenced to Coulomb rather than strong interactions [3], which motivates our measurement of isospin breaking in ^{47}K decay.

* behr@triumf.ca

II. THEORY AND METHODS

A. Isospin-forbidden β decay

In the angular distribution for allowed I=1/2 β decay in terms of lepton momentum p and energy E [4]:

$$dW = F(E,Z) p E p_\nu E_\nu \left(1 + a \frac{\vec{p_\beta}}{E_\beta} \cdot \frac{\vec{p_\nu}}{E_\nu} + \hat{I} \cdot \left(A_\beta \frac{\vec{p_\beta}}{E_\beta} + B_\nu \frac{\vec{p_\nu}}{E_\nu}\right)\right), \tag{1}$$

isospin-suppressed Fermi decay alters the correlation coefficients from their Gamow-Teller values:

$$a = \frac{y^2 - 1/3}{y^2 + 1}; A_\beta = A_{\beta GT} + f(M_F); B_\nu = -A_{\beta GT} + f(M_F) \tag{2}$$

with $y = g_V M_f / g_A M_{GT}$ and $f(M_F) = 2\sqrt{\frac{J}{J+1}} y$. The recoil asymmetry is then proportional to $A_\beta + B_\nu$, which vanishes when $M_F = 0$. (Analytic expressions for the proportion, which are possible if the Fermi function is set to unity, are given in Refs. [5, 6]: we compare here entirely to numerical simulations.)

B. Analog-antianalog mixing

The antianalog configuration has same spin and occupancy of spatial orbitals as the isobaric analog, but has total isospin reduced to $T = T_z$, with the antisymmetry of its wavefunction encoded differently between spin and isospin parts so that it is orthogonal to the analog state. Auerbach and Loc [1] using schematic wavefunctions write a closed-form expression for analog-antianalog Coulomb mixing for n_1 and n_2 excess neutrons over protons occupying orbitals j_1 and j_2:

$$\langle\bar{\mathcal{A}}|H_C|\mathcal{A}\rangle = \frac{\sqrt{n_1 n_2}}{2T}(\langle j_1|H_C|j_1\rangle - \langle j_2|H_C|j_2\rangle) \quad (3)$$

which for harmonic oscillator wavefunctions and a uniform charge distribution simplifies to

$$\langle\bar{\mathcal{A}}|H_C|\mathcal{A}\rangle \approx 0.35\frac{\sqrt{n_1 n_2}}{2T}\frac{Z}{A}(\langle j_1|r^2|j_1\rangle - \langle j_2|r^2|j_2\rangle) \quad (4)$$

$$\rightarrow 0.35\frac{\sqrt{n_1 n_2}}{2T}\frac{Z}{A^{2/3}}\text{MeV}, \quad (5)$$

when neutrons occupy two major shells differing by one $\bar{h}\omega$, in which case H_C is typically a factor of two larger. They validate this with calculations using RPA in demonstrative cases to achieve an accuracy of ∼20%. Predictions of H_C from Eq. 5 for cases of interest below include 160 keV for our case $^{47}_{19}\text{K}^{28}$ (with n_1=8 $f_{7/2}$ neutrons and n_2=1 $2s_{1/2}$ neutron), 301 keV for $^{57}_{28}\text{Co}^{29}$ (the 'isobaric parent analog' in the β^+ decay of ^{57}Ni), and 188 keV for $^{72}_{31}\text{Ga}^{41}$.

C. ^{47}K β^- decay to ^{47}Ca

The level scheme for ^{47}K is in Fig. 1. The ^{47}K I^π=$1/2^+$ ground-state has magnetic moment 1.933(9) μ_N [7], close enough to the proton μ to suggest a large fractional component of single-particle $2s_{1/2}$. The 80% branch to the $1/2^+$ 2560 keV state has log(ft)=4.82, which a literature shell-model calculation of the Gamow-Teller strength reproduces well, finding $\log(\text{ft})_{GT}$ = 4.39 [8]. This experimental $|M_{GT}|$=0.30 is considerably smaller than the single-particle $2s_{1/2}$ GT value of $\sqrt{3}$. We include in our simulations the 18.4±0.3% branch to the 2578 keV first excited $3/2^+$ state, and another 1.3% known to decay to five other $3/2^+$ states [9]: these can have no Fermi component and so simply dilute our measured A_{recoil}. Ref. [9] also observes 0.042% to first-forbidden branches– although these can have asymmetries near unity, we can safely ignore them at our achieved accuracy.

Because the first excited $3/2^-$ state is fed nearly all the time by γ's from the other transitions, direct β^- feeding is very difficult to constrain experimentally. A calculation of the first-forbidden nonunique fT value [8] would imply a branch of 0.25%: we choose not to attempt a correction, but note that including a 100% uncertainty from an 0.25% branch with unit asymmetry would not perturb our tabulated asymmetry uncertainties from the 80±2% branch below.

For pure Gamow-Teller decay, the beta asymmetry $A_{\beta GT}$=-2/3 for the $1/2^+ \rightarrow 1/2+$ transition and +1/3 for the $1/2^+ \rightarrow 3/2^+$ transitions. The weighted average from the measured branches [9] is then $A_{\beta GT}$=-0.467 ± 0.020. We include this in our simulation of pseudoA_β below.

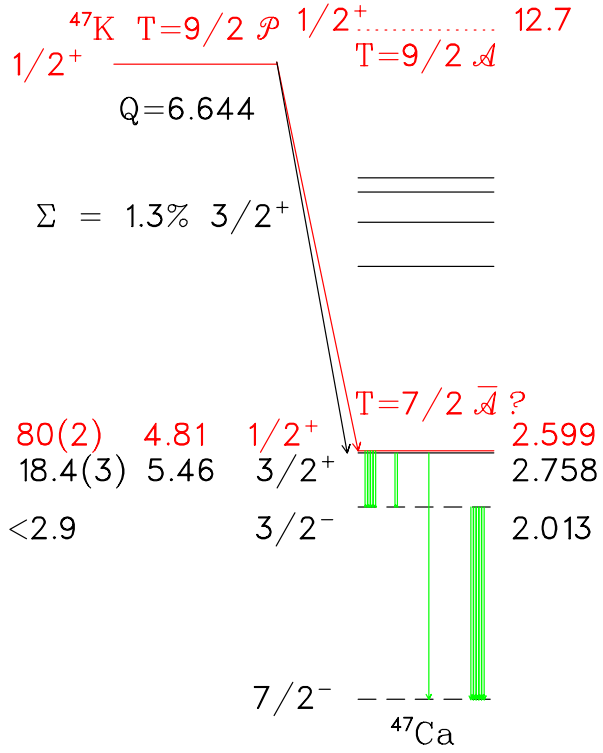

FIG. 1. Relevant allowed decay of ^{47}K, showing β^- branches >0.04%, log(ft), I^π, energy [MeV], and isospin T of the isobaric parent $\mathcal{P}$, analog $\mathcal{A}$, and possible antianalog $\bar{\mathcal{A}}$. Thickness of γ transitions >5% indicate intensity.

III. EXPERIMENT:

A. TRIUMF Neutral Atom Trap

Fig. 2 is a side view of the detection apparatus of TRIUMF's Neutral Atom Trap for β decay (TRINAT). Not shown is the collection trap from a vapour cell cube nor the push beams [10].

We trapped on average 500-1,000 ^{47}K atoms during the data-taking time. We used 250 mW of light from a Ti:Sapph to trap atoms in the collection trap, and similarly 200 mW to trap them in the detection trap. This light we found optimized the number of atoms trapped when tuned about 3 linewidths to the red of the $4S_{1/2}$ to $4P_{3/2}$ F=1 to F=2 transition, as measured with respect to the optical resonance measured by Ref. [7].

The repumping light on the F=0 to F=1 transition was about 50 mW from a tapered amplifier laser that was left on in the collection trap. In the detection trap, the repumping light was from the 0.15 mW/cm^2 optical pumping beams only, which were left on all of the time. This meant no repumping light at all for the transverse cooling between traps. Modest improvements on this configuration may trap more atoms in the future.

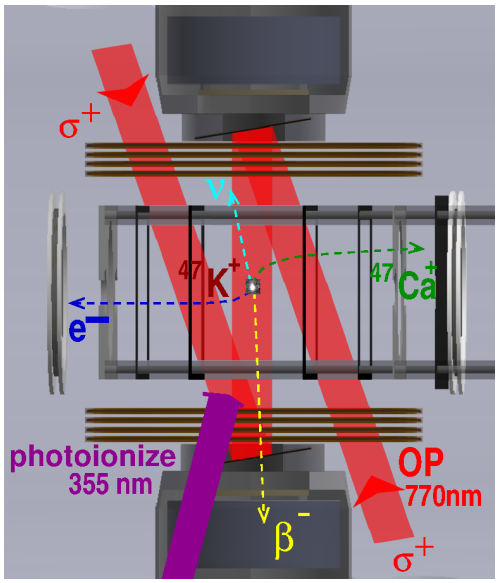

FIG. 2. TRINAT during the optical pumping time. Shown are β telescopes, mirrors for optical pumping light and its beams, magnetic field coils, electric field electrodes, and microchannel plates for electron and ion detection. A CMOS camera image of 1,000 trapped atoms is superimposed. Distance between trap cloud and ion MCP is 9.7 cm.

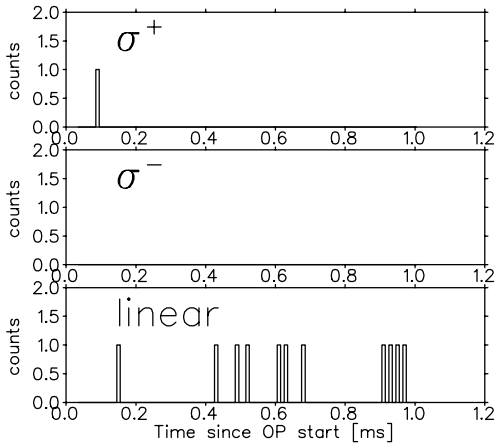

FIG. 3. Excited state population during the optical pumping time for circularly and linearly polarized light. See text for deduction of nuclear polarization.

B. Polarization by optical pumping

Details of optical pumping are very similar to our ^{37}K measurement [11]. Changes include much thinner pellicle mirrors along the optical pumping axis to reduce β straggling, made from 4 micron thick polyimide coated with 100 nm of Au. The optical pumping light quality is improved from 0.991 to closer to 0.996 Stokes parameter S_3.

We alternate 2.9 ms trapping with 1.1 ms optical pumping, during which we make the polarized beta decay measurements. During the polarization time, we apply circularly polarized light along the quantization axis. Once we start the OP cycle, atoms increase spin to maximum, then stop absorbing in the $S_{1/2}$ to $P_{1/2}$ transition used. If light is linearly polarized, atoms keep absorbing, and the atoms and nuclei remain roughly polarized.

When excited, 0.5 nsec pulsed from a 355 nm width laser have enough energy/photon to photoionize (a small fraction) of them, detected in the same ion microchannel-plate detector (MCP) used for the ^{47}Ca recoils from β decay. The photoions are distinguished by their time-of-Flight (TOF) and by their centre position, and we use them to determine average trap cloud sizes and positions when the MOT light is on.

The vanishing of photoion rate during the polarization time is then our probe of the atomic polarization quality. In Fig. 3 we show 11 photoions while linearly polarized (in about 1/4 the total time measured) and 1 photon circularly polarized. For spin-1/2 all the sub-level transitions have equal probabilities, making the deduced nuclear polarization simple to deduce, nearly independent of which nearly fully polarized states are excited. We deduce a fraction of nuclear polarization achieved for the decaying ^{47}K atoms of $P = \langle Iz \rangle / I = 0.96 \pm 0.04$.

We note that the optical pumping light was degrading smoothly in power during the data-taking of both circular and linearly polarized light by a factor of about four, caused by degradation of lithium niobate 3.3 GHz electro-optic modulators from photorefraction at about 4 mW of input optical power. We find from rate equation optical pumping simulations that the ratio of circular to linearly polarized photoions is similar as a function of power, so the average polarization reported describes the degree of polarization throughout the experiment. This ratio is also similar as a function of detuning to well within the accuracy we quote, important because we did not determine the resonance frequency other than optimizing the number of trapped atoms in the MOT.

C. Geometry and Detectors

An electric field is formed by a combination of low-Z glassy carbon and titanium electrodes to minimize β scattering. The field is calculated by standard finite element techniques to have average 650 V/cm, and after comparing with a full Monte Carlo simulation tracing trajectories in the detailed field, we found that taking this average as a uniform field is sufficiently accurate for our asymmetry simulations. The field collects ^{47}Ca ions produced in ^{47}K β^- decay to an MCP with 78 mm active diameter located 9.7 cm away. Decay by β^- naturally makes ^{47}Ca^{+1} ions. Additional low-energy atomic shakeoff electrons, which take an average of 6 ns to reach the opposite 40 mm diameter MCP, provide a starting trigger for the TOF of ^{47}Ca^2 and higher.

Critical to β detection is discriminating β's from γ's, because their ratio in ^{47}K decay is about 1 to 2. We use

the same 0.30 mm thick double-sided silicon strip detectors as Ref. [12], similarly requiring both X and Y strips above energy threshold and similar calibrated energy deposited. Our plastic 4x9cm scintillators for β^+ detection now use Silicon Photomultiplier (SiPM) readouts and are characterized in Ref. [13].

IV. RESULTS

Here we show results of 12 hours of beamtime, using 6x10^6/s mass-separated ^{47}K delivered from the TRIUMF/ISAC ISOL-type facility.

A. e$^-$–Recoil Coincidences

Our main channel is coincidences between decay recoils on the ion MCP and shakeoff electrons on the e$^-$ MCP (which correspond to ions with charge states +2 and higher). The TOF spectrum in Fig. 4 has contributions from ^{47}Ca charge states +2 through +7. Their asymmetry with respect to the polarization axis is shown to be nonzero in Fig. 5, directly implying a nonzero Fermi contribution to the $1/2^+ \rightarrow 1/2^+$ transition.

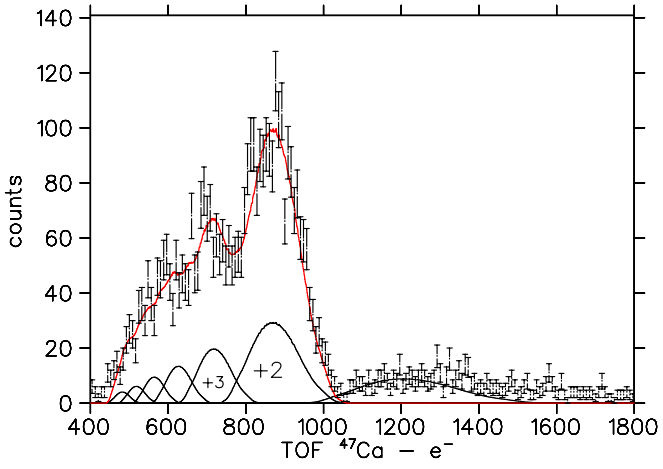

FIG. 4. Time-of-Flight (TOF) of ^{47}Ca ions triggered by shakeoff e$^-$.

We model this by a numerical integration of β and ν (Eqs. 1-2), with the resulting ^{47}Ca ions collected to the ion MCP by the 650 V/cm electric field. We find it adequate to include the momentum perturbation on the ^{47}Ca from a single 2 MeV γ subsequentially emitted isotropically — note emission of the dominant γ in Fig. 1 must be isotropic. The result is $y = +0.105 \pm 0.041$. Systematic uncertainties are listed in Table I.

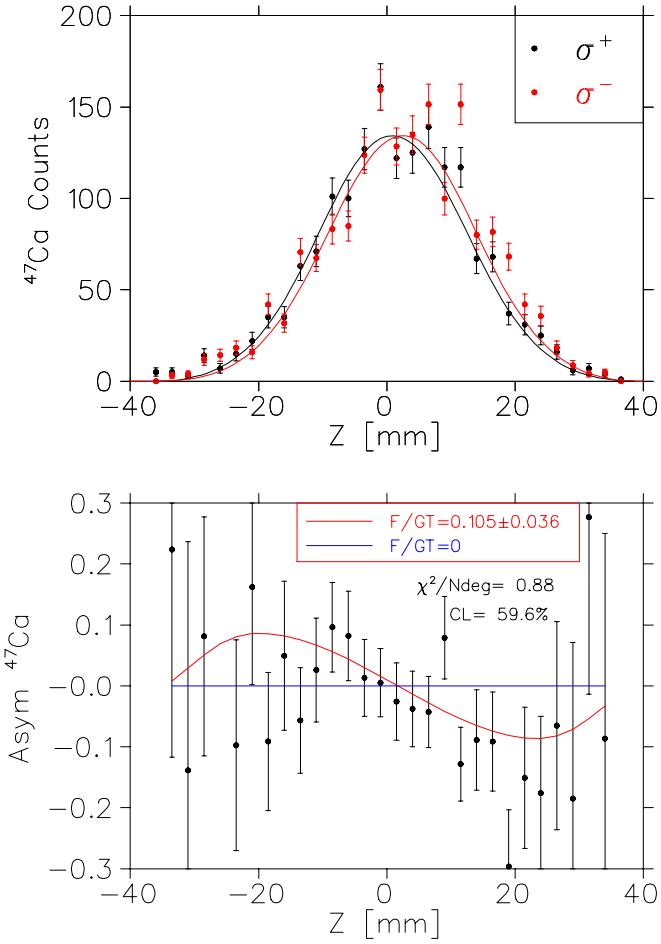

FIG. 5. Top: Distribution of shakeoff e$^-$ coincidences with ^{47}Ca$^{+2\ldots7}$ recoils along Z, the polarization axis, for the two polarizations. Bottom: The asymmetry of these distributions, i.e. the difference divided by the sum of the Top distributions. The nonzero asymmetry directly implies a nonzero Fermi contribution.

1. *Backgrounds from untrapped atoms and $^{47}Ca^{+1}$*

The vacuum-limited trap half-life of 10 sec and the $t_1/2$=17.5 sec of ^{47}K implies that more than half the nuclei decay after the atoms leave the trap. We have measured this background with 1 hour of data while deliberately ejecting atoms from the trap. We deduce a background of 6±4% of the events in the e$^-$–^{47}K channel, roughly flat in TOF in the region we use of +2 through +7 charge states, and include that background in our simulation. This is consistent with a small fraction of the untrapped atoms sticking to the glassy carbon electrodes slightly farther away from the trap– shakeoff electrons from other surfaces are excluded from the electron MCP by the electric field. Our β collimation is sufficient that we see backgrounds consistent with zero for the β-recoil channel considered below.

As β^- decay makes a +1 ion without further electron emission, the late-coming ^{47}Ca^{+1} in Fig. 4 must be co-

incidences with other prompt products. Hypothesizing all β's would produce a $^{47}Ca^{+1}$ distribution dominated by the ν asymmetry [14], we find an effective B_ν about half the value expected, indicating some MCP triggers from γ's. So the $\sim$ percent contribution to our TOF-selected recoils would make an $\sim$0.001 correction, which we tabulate as an uncertainty.

B. β–Recoil Coincidences Using PseudoA_β

We also measure β's in coincidence with ^{47}Ca recoils. If we measured ^{47}Ca recoils over all directions and momenta, this would be a measurement of A_β. However, some $^{47}Ca^{+1}$ ions with high transverse momenta do not impact the MCP, perturbing the asymmetry of β's in coincidence by a well-defined combination of the β-ν correlation and the ν asymmetry.

This observable, which we name pseudoA_β, we also model by numerical integration, including the effects of a single 2 MeV γ. We group the four combinations of β detector and polarization sign in pairs to cancel asymmetries. The results are in Fig. 6, where the different counting times of the 2 polarization states are included in the simulation and can be seen in the distributions. Numerical simulations for three values of M_F/M_{GT} show sensitivity to the asymmetry, along with the best fit. A single straight line for M_F=0 and hypothetical full collection of ^{47}Ca is shown, to indicate how the asymmetries are distorted from A_β from restrictions on the ^{47}Ca collection. The significantly smaller difference in asymmetry for positive vs. negative Z is due to an 0.5 mm displacement in the trap position along the Z-axis and subsequent change in ^{47}Ca collection, and is well-reproduced by the simulation.

We note that the sign of A_β is determined from this observable. We use this to determine the sign of our spin polarization, as we do not measure the absolute handedness of circularly polarized light.

To deduce a Fermi contribution from pseudoA_β requires more precision and accuracy than $A_{\rm recoil}$, because

TABLE I. Systematic uncertainties. Both observables are statistics dominated. NA denotes not applicable

Source	$A_{\rm recoil}$	pseudoA_β
$A_{\rm recoil}$ bkg 6±4%	0.014	< 0.002
Polarization 0.96±0.04	0.004	0.023
β^- Branching ratio	0.002	0.022
Weak magnetism	0.0006	0.0003
Fit range in Z ±20 to 34 mm	0.012	NA
$^{47}Ca^{+1}$ percent bkg	0.001	NA
$^{47}Ca^{+N}$ distribution from TOF	< 0.0005	NA
E field	negligible	0.025
Backscatter correction -0.012±20%	NA	0.0024
Fit statistics	0.037	0.082
Total	0.041	0.091

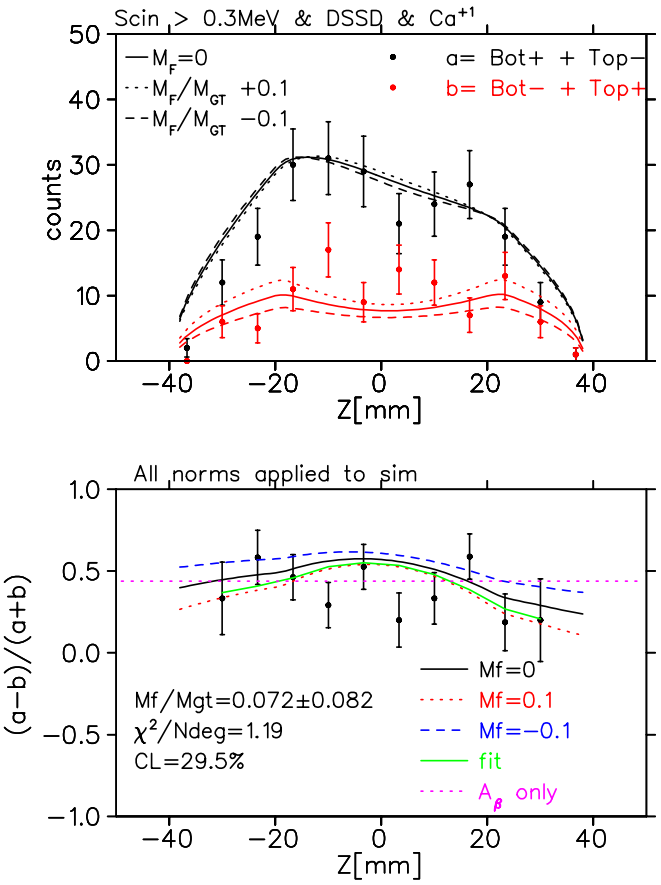

FIG. 6. Similar to Fig. 2, but for β-$^{47}Ca^{+1,2,3,4}$ coincidences.

we must distinguish between the experimental value and the nonzero theoretical value of A_β=-0.467 assuming pure Gamow-Teller transition. E.g. the polarization uncertainty contributes more to this observable. The uncertainties are summarized in Table I. Based on our previous ^{37}K A_β measurement [12], we scale our experimental value by 1/1.023 to approximately account for backscatter, assigning here a more generous uncertainty here of 20% because we have not done full simulations of geometry changes.

The result from pseudoA_β, y=0.072±0.091, is consistent in sign with $A_{\rm recoil}$, but with larger uncertainty.

1. *Recoil order corrections.*

We use Ref. [15, 16] for the exact correction from the recoil kinetic energy and the 1st-order in recoil correction from weak magnetism b_W. Assuming the wavefunction of initial and final $1/2^+$ states is an $s_{1/2}$ nucleon, b_W has no orbital angular momentum contribution and becomes the nucleon value [17]: the first-class induced tensor d_I also vanishes for $s_{1/2}$. Similarly assuming single-particle $s_{1/2} \rightarrow d_{3/2}$ for the 20% branches to $3/2^+$ states, the orbital correction to b is zero if l changes; here we can ignore

potentially nonzero d_I and 2nd-order in recoil corrections because of the 20% fraction. The recoil corrections increase our deduced $A_{\rm recoil}$ by 0.0025, 0.0012 from b_W to which we assign 50% uncertainty. Similarly, b_W changes pseudoA_β by 0.0006, to which we also assign 50% uncertainty.

C. Result and Isospin breaking

Our weighted average of results from $A_{\rm recoil}$ and pseudoA_β is then $y = g_V M_F/g_A M_{GT}$= 0.099±0.037 for the $1/2^+$ to $1/2^+$ transition.

Given the measured log(ft) of 4.82 (which implies $g_A M_{GT}$= 0.305), we deduce $|M_F|$= 0.030±0.011 (assuming we do not know the sign of M_{GT}). and the standard model value of g_V = 1.00). To compare to other nuclei thought to be dominated by analog-antianalog mixing, we use a first-order perturbation theory expression from the literature, including the standard ladder operator result for isospin [18, 19]: $M_F = \frac{\langle A|H_C|\bar{A}\rangle}{\Delta E}\sqrt{(T\mp T_z)(T\pm T_z+1)}$ (upper vs. lower sign for β^- vs. β^+), along with the measured analog-antianalog splitting ΔE = 10.1 MeV [20], to deduce a Coulomb matrix element $|H_C|$= 93 ± 36 keV.

This Coulomb matrix element is over half of the 160 keV prediction of analog-antianalog mixing. We attribute this to the simple structure of nearly-doubly magic ^{47}Ca and its single $1/2^+$ state. That this is not the full prediction suggests the state is somewhat more complex than the antianalog. Since the antianalog has determined spin equal to the analog, it seems unlikely the antianalog configuration is contained in other states.

Many β decays in such systems have much smaller Coulomb matrix elements and M_F. Ref. [1] suggests the antianalog configuration is often fragmented among many states. Fig. 7, a plot of literature measurements of y [18], suggests that M_F can maintain a substantial fraction of M_{GT} even as $|M_{GT}|$ decreases by two orders of magnitude, suggesting general decrease of both with the complexity of nuclear states. At least two other cases with large M_F and H_C, ^{57}Ni and ^{71}Ga, like ^{47}Ca have low-lying states of opposite parity and thus are also close to shell closures, consistent with Ref. [1] prediction of larger H_C if two major shells are occupied. The $\beta+$ decay of ^{56}Co in constrast has a strikingly small H_C, since its relevant isobaric parent $\mathcal{P}$ ^{56}Fe has excess neutrons spanning the N=28 shell closure: one explanation would be fragmentation of the $\bar{A}$ configuration.

Ref. [3] advocates a time-reversal measurement in ^{134}Cs, which has a very slow M_{GT} transition and small Coulomb matrix element (and a measurement was similarly pursued in ^{56}Co [27]). However, if isovector TOPE nucleon-nucleon [28] matrix elments have similar dependence on nuclear complexity, a faster Gamow-Teller decay like ^{47} would also be a favourable system for time-reversal decay.

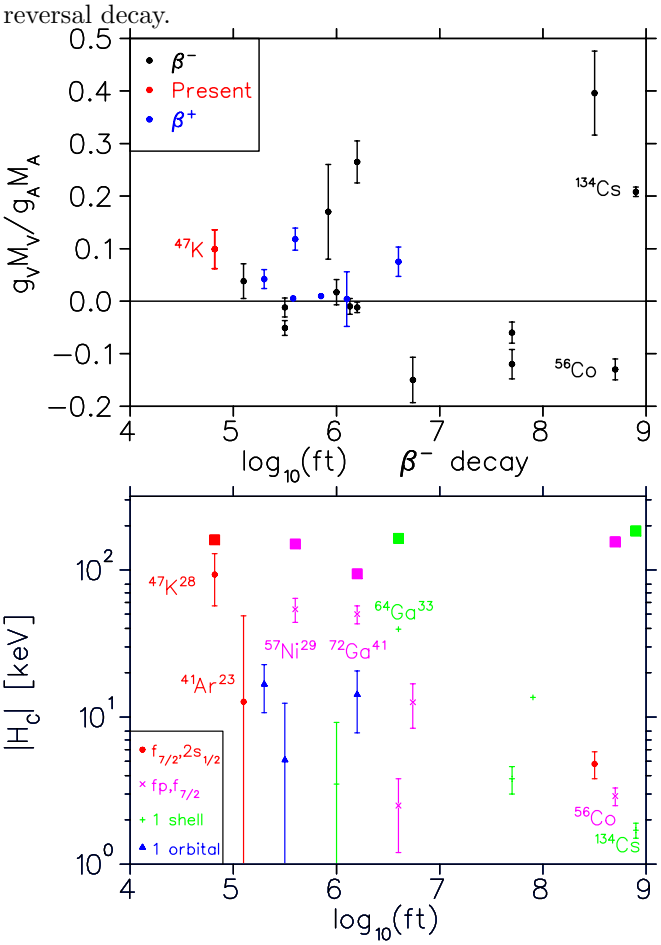

FIG. 7. Ratio of Fermi to Gamow-Teller matrix elements y as a function of log(ft) for isospin-suppressed transitions from Refs. [18, 21–26]. The magnitude of the ratio can remain ∼0.1 even as M_{GT} falls two orders of magnitude. Bottom: Deduced Coulomb matrix elements H_C from isospin-forbidden β decay experiments. Solid squares show calculation of $\mathcal{A}-\bar{\mathcal{A}}$ mixing from Eqs. 3 and 4 [1]. H_C can be large when excess neutrons over protons occupy major shells.

V. CONCLUSION

For the ^{47}K β^- $1/2^+\rightarrow 1/2^+$ transition, we have measured the ratio of Fermi to Gamow-Teller matrix elements y=0.099±0.037. Interpreted as analog-antianalog mixing in the progeny ^{47}Ca, this result implies a relatively large effective Coulomb mixing matrix element magnitude 93±35 keV. A large matrix element of 160 keV is generated for ^{47}Ca from analog-antianalog mixing, as its excess neutrons over protons occupy two major shells, $f_{7/2}$ and sd, with naturally different Coulomb energies [1]. The large fraction observed of that prediction we attribute to the existence of only one $1/2^+$ state in the nearly-doubly-magic ^{47}Ca.

[1] N. Auerbach and M. L. Bui, Coulomb corrections to fermi beta decay in nuclei, Nuclear Physics A **1027**, 122521 (2022).

[2] M. Simonius, Constraints on parity-even time reversal violation in the nucleon-nucleon system and its connection to charge symmetry breaking, Phys. Rev. Lett. **78**, 4161 (1997).

[3] A. Barroso and R. Blin-Stoyle, A test for time-reversal violation in allowed isospin-hindered beta-decay, Physics Letters B **45**, 178 (1973).

[4] J. Jackson, S. Treiman, and H. Wyld, Coulomb corrections in allowed beta transitions, Nuclear Physics **4**, 206 (1957).

[5] J. R. A. Pitcairn, D. Roberge, A. Gorelov, D. Ashery, O. Aviv, J. A. Behr, P. G. Bricault, M. Dombsky, J. D. Holt, K. P. Jackson, B. Lee, M. R. Pearson, A. Gaudin, B. Dej, C. Höhr, G. Gwinner, and D. Melconian, Tensor interaction constraints from β-decay recoil spin asymmetry of trapped atoms, Phys. Rev. C **79**, 015501 (2009).

[6] S. B. Treiman, Recoil effects in k capture and β decay, Phys. Rev. **110**, 448 (1958).

[7] F. Touchard, P. Guimbal, S. Büttgenbach, R. Klapisch, M. De Saint Simon, J. Serre, C. Thibault, H. Duong, P. Juncar, S. Liberman, J. Pinard, and J. Vialle, Isotope shifts and hyperfine structure of 38–47k by laser spectroscopy, Physics Letters B **108**, 169 (1982).

[8] P. Choudhary, A. Kumar, P. C. Srivastava, and T. Suzuki, Structure of ^{46,47}Ca from the β^- decay of ^{46,47}K in the framework of the nuclear shell model, Phys. Rev. C **103**, 064325 (2021).

[9] J. K. Smith, A. B. Garnsworthy, J. L. Pore, C. Andreoiu, A. D. MacLean, A. Chester, Z. Beadle, G. C. Ball, P. C. Bender, V. Bildstein, R. Braid, A. D. Varela, R. Dunlop, L. J. Evitts, P. E. Garrett, G. Hackman, S. V. Ilyushkin, B. Jigmeddorj, K. Kuhn, A. T. Laffoley, K. G. Leach, D. Miller, W. J. Mills, W. Moore, M. Moukaddam, B. Olaizola, E. E. Peters, A. J. Radich, E. T. Rand, F. Sarazin, C. E. Svensson, S. J. Williams, and S. W. Yates, Spectroscopic study of ^{47}Ca from the β^- decay of ^{47}K, Phys. Rev. C **102**, 054314 (2020).

[10] T. B. Swanson, D. Asgeirsson, J. A. Behr, A. Gorelov, and D. Melconian, Efficient transfer in a double magneto-optical trap system, J. Opt. Soc. Am. B **15**, 2641 (1998).

[11] B. Fenker, J. A. Behr, D. Melconian, R. M. A. Anderson, M. Anholm, D. Ashery, R. S. Behling, I. Cohen, I. Craiciu, J. M. Donohue, C. Farfan, D. Friesen, A. Gorelov, J. McNeil, M. Mehlman, H. Norton, K. Olchanski, S. Smale, O. Thériault, A. N. Vantyghem, and C. L. Warner, Precision measurement of the nuclear polarization in laser-cooled, optically pumped 37k, New Journal of Physics **18**, 073028 (2016).

[12] B. Fenker, A. Gorelov, D. Melconian, J. A. Behr, M. Anholm, D. Ashery, R. S. Behling, I. Cohen, I. Craiciu, G. Gwinner, J. McNeil, M. Mehlman, K. Olchanski, P. D. Shidling, S. Smale, and C. L. Warner, Precision measurement of the β asymmetry in spin-polarized ^{37}K decay, Phys. Rev. Lett. **120**, 062502 (2018).

[13] M. Ozen, J. A. Behr, M. Khoo, F. Klose, A. Gorelov, and D. Melconian, Lineshape response of plastic scintillator to pair production of 4.44 mev γ's, Nuclear Instruments and Methods in Physics Research Section A: Accelerators, Spectrometers, Detectors and Associated Equipment **1055**, 168490 (2023).

[14] D. Melconian, J. Behr, D. Ashery, O. Aviv, P. Bricault, M. Dombsky, S. Fostner, A. Gorelov, S. Gu, V. Hanemaayer, K. Jackson, M. Pearson, and I. Vollrath, Measurement of the neutrino asymmetry in the β decay of laser-cooled, polarized ^{37}k, Physics Letters B **649**, 370 (2007).

[15] B. R. Holstein, Recoil effects in allowed beta decay: The elementary particle approach, Rev. Mod. Phys. **46**, 789 (1974).

[16] B. R. Holstein, Erratum: Recoil effects in allowed beta decay: The elementary particle approach, Rev. Mod. Phys. **48**, 673 (1976).

[17] X. B. Wang and A. C. Hayes, Weak magnetism correction to allowed β decay for reactor antineutrino spectra, Phys. Rev. C **95**, 064313 (2017).

[18] S. Bhattacherjee, S. Mitra, and H. Padhi, Fermi matrix elements in allowed beta transitions in 56co, 58co and 134cs, Nuclear Physics A **96**, 81 (1967).

[19] S. D. Bloom, Isotopic-spin conservation in allowed β-transitions and coulomb matrix elements, Il Nuovo Cimento **32**, 1023 (1964).

[20] T. Burrows, Nuclear data sheets for a = 47, Nuclear Data Sheets **108**, 923 (2007).

[21] L. G. Mann, D. C. Camp, J. A. Miskel, and R. J. Nagle, New measurements of β-circularly-polarized γ angular-correlation asymmetry parameters in allowed β decay, Phys. Rev. **139**, AB2 (1965).

[22] J. Atkinson, L. Mann, K. Tirsell, and S. Bloom, Coulomb matrix elements from $\beta-\gamma$(cp) correlation measurements in 57ni and 65ni, Nuclear Physics A **114**, 143 (1968).

[23] H. Behrens, Messung des asymmetrie-koeffizienten der β − γ-zirkularpolarisationskorrelation an erlaubten β-übergängen, Z. Physik **201**, 153 (1967).

[24] J. Markey and F. Boehm, Fermi—gamow-teller interference in ^{56}Co decay, Phys. Rev. C **26**, 287 (1982).

[25] N. Severijns, D. Vénos, P. Schuurmans, T. Phalet, M. Honusek, D. Srnka, B. Vereecke, S. Versyck, D. Zákoucký, U. Köster, M. Beck, B. Delauré, V. Golovko, and I. Kraev, Isospin mixing in the $t = 5/2$ ground state of ^{71}As, Phys. Rev. C **71**, 064310 (2005).

[26] P. Schuurmans, J. Camps, T. Phalet, N. Severijns, B. Vereecke, and S. Versyck, Isospin mixing in the ground state of 52mn, Nuclear Physics A **672**, 89 (2000).

[27] F. P. Calaprice, S. J. Freedman, B. Osgood, and W. C. Thomlinson, Test of time-reversal invariance in the beta decay of ^{56}Co, Phys. Rev. C **15**, 381 (1977).

[28] P. Herczeg, The general form of the time-reversal noninvariant internucleon potential, Nuclear Physics **75**, 655 (1966).